Rangeland Ecology & Management 68 (2015) 18–28

Contents lists available at ScienceDirect

Rangeland Ecology & Management

journal homepage: http://www.elsevier.com/locate/rama

Mapping and Monitoring Cheatgrass Dieoff in Rangelands of the Northern Great Basin, USA☆,☆☆,★

Stephen P. Boyte [a,*], Bruce K. Wylie [b], Donald J. Major [c]

[a] Senior Scientist, Stinger Ghaffarian Technologies, Inc., contractor to the U.S. Geological Survey (USGS) Earth Resources Observation Science (EROS) Center, Sioux Falls, SD 57198, USA
[b] Research Physical Scientist USGS EROS Center, Sioux Falls, SD 57198, USA
[c] At the time of research, D.J. Major has re-assumed his role as a Fire and Landscape Ecologist, Bureau of Land Management, Boise, ID, 83709, USA

ARTICLE INFO

Article history:
Received 7 January 2014
Accepted 6 August 2014

Keywords:
Bromus tectorum
ecological models
invasive species
land cover change
MODIS
Snake River Plain

ABSTRACT

Understanding cheatgrass *(Bromus tectorum)* dynamics in the Northern Great Basin rangelands, USA, is necessary to effectively manage the region's lands. This study's goal was to map and monitor cheatgrass performance to identify where and when cheatgrass dieoff occurred in the Northern Great Basin and to discover how this phenomenon was affected by climatic, topographic, and edaphic variables. We also examined how fire affected cheatgrass performance. Land managers and scientists are concerned by cheatgrass dieoff because it can increase land degradation, and its causes and effects are not fully known. To better understand the scope of cheatgrass dieoff, we developed multiple ecological models that integrated remote sensing data with geophysical and biophysical data. The models' R^2 ranged from 0.71 to 0.88, and their root mean squared errors (RMSEs) ranged from 3.07 to 6.95. Validation of dieoff data showed that 41% of pixels within independently developed dieoff polygons were accurately classified as dieoff, whereas 2% of pixels outside of dieoff polygons were classified as dieoff. Site potential, a long-term spatial average of cheatgrass cover, dominated the development of the cheatgrass performance model. Fire negatively affected cheatgrass performance 1 year postfire, but by the second year postfire performance exceeded prefire levels. The landscape-scale monitoring study presented in this paper helps increase knowledge about recent rangeland dynamics, including where cheatgrass dieoffs occurred and how cheatgrass responded to fire. This knowledge can help direct further investigation and/or guide land management activities that can capitalize on, or mitigate the effects of, cheatgrass dieoff.

Introduction

Ecosystems change when non-native species invade, and these changes can be long lasting and substantial. For more than 100 years, cheatgrass (*Bromus tectorum* L.), a winter annual grass, has invaded western U.S. rangelands (Mack and Pyke, 1983). As this invasion has advanced, it has become geographically extensive and profuse in areas, especially in the Snake River Plain and the Great Basin. Bradley and Mustard (2005) estimated that 7%, or 20 000 km^2, of Great Basin land cover is dominated by cheatgrass; the authors of this paper documented, on the ground, cheatgrass coverage greater than 85% in spring 2014 at the local level in the Snake River Plain. The effect of cheatgrass has been exceptionally profound in the Northern Great Basin region, where it has helped cause a dramatic increase in fire frequencies and severities (Whisenant, 1990; Balch et al., 2013). This altered fire regimen contributed to the degradation of rangelands where large areas have been converted from diverse, species-rich native systems to systems where cheatgrass dominated. Our study area (defined more completely in the Methods section) included all of the Northern Basin and Range and the Snake River Plain ecoregions (Commission on Environmental Cooperation www.cec.org) but also included parts of ecoregions contiguous to these two. We identify the primary two ecoregions as the Northern Great Basin; however, analysis was conducted on all unmasked areas.

Changed disturbance regimens present new challenges and make it difficult for land managers to develop timely adaptive strategies. The cheatgrass invasion and its challenges have been well documented (Young et al., 1987; Whisenant, 1990; Mack, 2011), but research regarding cheatgrass and its effects on the ecosystems it has invaded

☆ Research was funded by USGS Land Remote Sensing, USGS Land Change Science, Bureau of Land Management, and The Department of the Interior Northwest Climate Science Center.
☆☆ Work performed under USGS contract G10PC00044 (Boyte).
★ Any use of trade, product, or firm names is for descriptive purposes only and does not imply endorsement by the U.S. Government.
* Correspondence: Stephen P. Boyte, SGT, Inc., USGS EROS Center, Sioux Falls, SD 57198, USA.
E-mail address: sboyte@usgs.gov (S.P. Boyte).

http://dx.doi.org/10.1016/j.rama.2014.12.005
1550-7424/

has continued (Chambers et al., 2007; Bromberg et al., 2011; Goergen et al., 2011; Baynes et al., 2012). Another challenge recently observed (since at least 2003) in the Great Basin by a longtime Bureau of Land Management (BLM) employee is cheatgrass dieoff (M. Zielinski, personal communication, September, 2010). We defined cheatgrass dieoff as a substantial reduction, or a complete lack, of cheatgrass productivity during years of adequate precipitation in previously invaded stands. Researchers, land managers, and land owners have developed various hypotheses for causes of cheatgrass dieoff (Salo, 2011), suspecting the black fingers of death (*Pyrenophora semeniperda*), a cheatgrass seed pathogen (Beckstead et al., 2007; Meyer et al., 2007; Beckstead et al., 2011), to be a possible cause of dieoff. Cheatgrass dieoff might be seen as a positive development in our study area, but it presents tangible problems that demand more understanding. These problems include accelerated soil erosion, loss of early spring forage for livestock and wildlife, the introduction of weed species new to these dieoff areas, and unknown recovery pathways. Also, black fingers of death can spill over from cheatgrass seeds to infect seeds of co-occurring native grasses like Indian ricegrass (*Achnatherum hymenoides* [Roem. & Schult.] Barkworth), squirreltail (*Elymus elymoides* [Raf.] Swezey), needle and thread (*Hesperostipa comata* [Trin. & Rupr.] Barkworth), Sandberg's blue grass *(Poa secunda* J. Presl), and bluebunch wheatgrass (*Pseudoroegneria spicata* [Pursh] Á. Löve) (Beckstead et al., 2010).

The goal of this study was to gain a regional perspective on cheatgrass dieoff in the Northern Great Basin and surrounding areas from 2000–2010. To achieve this goal, we implemented the dynamic monitoring of ecosystem performance method (Wylie et al., 2008; Gu et al., 2012; Wylie et al., 2012; Rigge et al., 2013), using a coarse-scale remote sensing product. This method isolated the effects of weather and site potential from the effects of disturbances, allowing disturbances to be displayed as underperforming ecosystem anomalies, or possible cheatgrass dieoff. We integrated the remote sensing data into regression-tree models with biophysical and geophysical variables, weather data, and three categorical datasets that delineated land cover, ecoregions, and potential vegetation cover. These datasets were used to classify cheatgrass performance and, thereby, map possible cheatgrass dieoff. In the process of preparing data to implement the dynamic monitoring of ecosystem performance, we contrasted cheatgrass phenology with the phenology of other Northern Great Basin vegetation types, which allowed us to identify cheatgrass presence and estimate its percent cover. Annual production of cheatgrass is much more sensitive to annual precipitation than is native plant production (Bradley and Mustard, 2005); consequently, we focused on the unique phenology of cheatgrass (Link et al., 1990; Peterson, 2005; Kokaly, 2011) to form our cheatgrass performance study. This method can help locate possible cheatgrass dieoffs in the Northern Great Basin because these dieoffs are disturbances independent of weather, and, by including weather data in our models, the models are detrended for weather. These models output ecosystem performance data that are expected in a given year at a given site *excluding* effects from disturbances or management activities. Therefore we developed a time series that separates ecosystem performance anomalies (EPAs) (underperforming or overperforming) from each other and from areas of normal performance.

We assumed cheatgrass underperformance to be an indicator of possible cheatgrass dieoff, and our data and analysis methods were useful to annually assess and monitor cheatgrass performance. The objectives of this study included 1) developing a time series of annual cheatgrass performance map products (2000–2010); 2) developing cheatgrass performance persistent anomaly and trend maps; 3) comparing cheatgrass persistent anomalies to topographic, edaphic, and climate variables; and (4) comparing prefire and postfire cheatgrass EPA values.

Methods

Study Area

The study area included about 505 000 km^2 in parts of seven U.S. western states: California, Idaho, Montana, Nevada, Oregon, Utah, and Wyoming. Plains, rolling hills, scattered mountain ranges, alluvial fans, and valleys make up this area (U.S. Department of Interior, 2010). The average elevation equals 1 679 m and elevations range from 549 to 4 061 m. The 30-year (1981–2010) precipitation mean equaled 434 mm per year. For the same time period, the mean minimum temperature equaled -11°C and the mean maximum temperature equaled 13.8°C (PRISM Climate Group, Oregon State University). Seasonal wetlands and evaporational basins are numerous because much of the area does not drain externally.

The study area was composed of sagebrush steppe, juniper woodlands, salt-desert scrub, playas, subalpine coniferous forests, and alpine environments. Many vegetation types were present and included native perennial grasses such as Thurber's needlegrass (*Achnatherum thurberianum* [Piper] Barkworth), Sandberg's bluegrass, bluebunch wheatgrass, and Idaho fescue (*Festuca idahoensis* Elmer). Several shrub types and evergreen trees were common. Most common among shrub types was a complex of big sagebrush that included Wyoming big sagebrush (*Artemisia tridentata* Nutt. ssp. *wyomingensis*), Mountain big sagebrush (*A. t.* Nutt. ssp. *vaseyana*), and Basin big sagebrush (*A. t.* Nutt. ssp. *tridentata*). Other shrubs were bitterbrush (*Purshia tridentata* [Pursh] DC) (West and Young, 2000), rabbitbrush (*Chrysothamnus Nutt.*), and little sagebrush (*A. arbuscula* Nutt.). Livestock grazing continued to be an important activity in the study area and has caused major changes in the area's vegetation structure and function (West and Young, 2000). Other economic activities included outdoor recreation, mining, and forestry (Wiken et al., 2011). A large percentage of these lands were managed by federal agencies.

Data

eMODIS NDVI

This study used enhanced Moderate Resolution Imaging Spectroradiometer (eMODIS) Normalized Difference Vegetation Index (NDVI) data at 250-m spatial resolution. eMODIS NDVI, a derivative of NASA's MODIS product, is useful for conducting remote sensing vegetation studies because its temporal resolution is fine enough to effectively capture plant phenologies, especially short-lived annuals like cheatgrass. NDVI is created using the MODIS red (620–670 nm) and near-infrared (NIR) bands (841–876 nm) in a simple equation (Eq. 1). eMODIS NDVI delivers 7-day composites created from the most recent 7 days of acquisitions, and then an algorithm selects the best pixel from the acquisitions; the algorithm filters through input surface reflectance that flags clouds, snow cover, and low-view angles (Jenkerson et al., 2010). A temporal smoothing program (Swets et al., 2000) was applied to the data to remove effects of residual clouds that can lead to artificially low values. Also, we subtracted a baseline value of 0.10 from the eMODIS NDVI to compensate for bare ground and dormant vegetation.

$$NDVI=(NIR-Red)/(NIR+Red) \quad (1)$$

eMODIS NDVI-derived Datasets

Four annual datasets were generated from eMODIS NDVI data: 1) integrated cheatgrass growing season NDVI; 2) integrated summer NDVI periods; 3) cheatgrass indices; and 4) cheatgrass start of spring growth. Cheatgrass growing season NDVI was spatially and

temporally dynamic, and the start of its integration period was dependent on cheatgrass start of spring growth. Therefore to help define annual cheatgrass growing season NDVI, we created dynamic annual cheatgrass start of spring growth datasets (described in the next section) to determine when to start the growing season NDVI integration period for each pixel. Once annual growing season NDVI was established, we parsed each growing season NDVI dataset into one of four 8-week periods to coincide with cheatgrass start of spring growth.

Cheatgrass senescence, like cheatgrass growing season NDVI, was spatially and temporally dynamic, so the annual summer integration periods were designed to capture NDVI values when cheatgrass was not green but most other vegetation types were green. Cheatgrass senescence normally begins before or around middle June in the study area, so we integrated annual summer weekly composites[1] starting on 14 June at the earliest, to 20 June, at the latest, for 5 weeks to capture cheatgrass senescence and contrast it with the greenness of other vegetation types. Kokaly (2011) described a technique to identify cheatgrass using Landsat data. In pixels where spring NDVI values were much higher than midsummer NDVI values, he noted that these NDVI values manifested "the vegetation growth cycle of cheatgrass." We modified his technique using a simple equation to develop annual cheatgrass indices that provided a rough estimate for annual cheatgrass percent cover (Eq. 2).

$$\textit{Cheatgrass Index} = (\text{growing season NDVI} - \textit{Summer}) / (\text{growing season NDVI} + \textit{Summer}) \quad (2)$$

Cheatgrass Start of Spring Growth

A regression-tree model that predicts annual cheatgrass start of spring growth on the basis of cheatgrass-dominated pixel characteristics (Boyte et al., 2013) was built. The model was trained on 939 points where either 2001 data or 2006 data from the Nevada Natural Heritage Program[4] indicated that 30% or more cheatgrass or annual grass cover existed. We chose this threshold to increase confidence that training pixels would exhibit NDVI values characteristic of cheatgrass. Outside of agricultural areas, early spring NDVI values greater than 0.30 in the Northern Great Basin normally indicate active cheatgrass growth (Gu et al., 2010); consequently, we examined eMODIS NDVI weekly composite values at each training point and identified when the NDVI value exceeded 0.30 for at least 6 consecutive weeks. These consecutive weekly periods should coincide with and represent the cheatgrass sustained spring growing season. The first week of the weekly composites that was identified as the start of growth for each pixel was used as the dependent variable in the regression-tree model. Independent variables were selected after carefully testing model accuracies using different combinations of prospective drivers of cheatgrass start of spring growth. This dataset was used only to determine when to start the growing season NDVI integration period for every pixel for each year. It was not used as an input into the regression-tree model that estimated cheatgrass percent cover.

Actual Cheatgrass Performance (ACP) Model

The following datasets were processed and used in a regression-tree model to help spatially and temporally extrapolate the 2001 and 2006 cheatgrass percent cover maps to annual cheatgrass percent cover for 2000–2010.

1) The percent cover data, used as the dependent variable, were downloaded at 30-m spatial resolution, spatially averaged, and resampled to 250 m using a bilinear interpolation function (Peterson, 2005, 2007).
2) Elevation, steep slope, and aspect datasets were developed from the National Elevation Dataset[2] (NED). The compound topographic index (CTI), a wetness index, was a product of slope and upstream contributions (Chaplot and Walter, 2003). These 30-m datasets were spatially averaged and resampled to 250 m using bilinear interpolation. Slopes exceeding 8.5% were classified as steep. North-facing slopes equaled azimuths between 315° and 45°, and south-facing slopes equaled azimuths between 135° and 225°.
3) A latitude dataset was developed to approximate changing latitudes. The dataset measured meters north of the latitude of origin at 23° north in the Albers Equal Area Conic U.S. Geological Survey (USGS) version projection.
4) Categorical datasets were used to help define model rules. These datasets are the 2001 National Land Cover Database[3] (NLCD), masked to show only shrub or grassland, the Natural Resources Conservation Service Major Land Resource Area[4] (MRLA), and LANDFIRE environmental site potential.[5] These 30-m datasets were put through a moving 9 x 9 filter where the most commonly occurring value was returned. The datasets were resampled to 250 m.
5) Start of season time (SOST) was an eMODIS NDVI 250-m derived dataset that employs a dynamic moving average method (Reed et al., 1994; White et al., 2009). SOST was the day of year when the smoothed NDVI time series crossed a curve established from moving average models with an introduced time lag of 36 weekly composites, indicating that NDVI values were beginning to trend upward. We assumed SOST captures variations between years and across space in the ACP model and growing season NDVI.
6) Soil Survey Geographic Database[6] (SSURGO) datasets were used for available water capacity (AWC) and soil organic carbon (SOC). AWC was measured in centimeters, and SOC was measured as $kg \cdot m^{-2}$. Both datasets were measured at 0- to 30-cm depths. The datasets were spatially averaged and resampled to 250 m using bilinear interpolation.

Expected cheatgrass performance (ECP) model

1) In the ECP model, we predicted ACP, so the ACP dataset served as the dependent variable.
2) Site potential represented the long-term spatial average of ACP. To create site potential, we calculated the median value of ACP for each pixel from 2000–2010. Then, on a pixel-by-pixel basis, we calculated the mean of all values above that median value. The mean-above-the-median dataset served as site potential. Site potential should not have overemphasized singular anomalous events.
3) PRISM monthly weather data (precipitation, temperature maximum, and temperature minimum) for each year (2000–2010) were downloaded (http://www.prism.oregonstate.edu/) at a 4-km spatial resolution, resampled to 250 m using bilinear interpolation, and then aggregated for the winter season (November, December, January, and February) or used in monthly time steps for October, March, April, and May.

[1] eMODIS NDVI weekly composites vary slightly year to year, so an exact date match between years is not possible.

[2] http://ned.usgs.gov.
[3] http://www.mrlc.gov/.
[4] http://soils.usda.gov/survey/geography/mlra/.
[5] http://www.landfire.gov/.
[6] http://soils.usda.gov.survey/geography/ssurgo/.

Modeling Processes

Actual Cheatgrass Performance (ACP)

To identify cheatgrass dieoff and understand dieoff dynamics, our modeling processes involved the development of a time series (2000–2010) of annual cheatgrass percent cover estimates, also known as actual cheatgrass performance (ACP). We predicted ACP using a rule-based, piecewise regression-tree model integrated with the geophysical data, biophysical data, three categorical datasets, and remote sensing data described earlier. The ACP model was trained on 35 988 points almost equally divided from each of the 2001 and 2006 datasets. The correlation coefficient of the 2001 dataset equaled 0.71 with a RMSE of 9.1%. The RMSE equaled 10% to 16% with 75% of field plots within 14% of field measurements for the 2006 dataset (Peterson, 2005, 2007). The ACP model was built on the western two-thirds of the study area and extrapolated to the eastern one-third. Training points were randomly stratified into four cheatgrass percent cover classes of nearly equal sizes. These classes were zero, 1 to 12, 13 to 25, and more than 25. We also limited training point locations on the basis of two spatial criteria:

- The land cover was classified as grassland/herbaceous or shrub by the 2001 NLCD (this limits training points to likely rangeland areas).
- Elevation equaled 2000 m or lower.

We stratified training points to ensure that rare, extreme values were accurately predicted, that our model was robust to a wide range of site and weather conditions, and that predictions had, at most, minor bias.

We used the Cubist rule-based, piecewise regression model to refine the rough estimates of cheatgrass percent cover provided by the cheatgrass indices described earlier. We chose this approach because regression-tree models uncovered causal relationships between independent and dependent variables (Wylie et al., 2007) and can be used to explain nonlinear biological relationships (Toms and Lesperance, 2003) by splitting the independent variables into branches that ended or continued on the basis of rules defined by the independent data (De'ath and Fabricius, 2000). When a rule's conditions were met, an associated multivariate linear model was created to predict a pixel value. A pixel that met more than one rule returned an average value of the associated regression predictions (RuleQuest, 2008).

Figure 1 illustrates the modeling process and data used to estimate cheatgrass percent cover. We built a predictive model using 3 committees and 100 rules. Committee models built successive piecewise regression models that improved on the errors of the previous model and constructed more interpretable maps. Each committee generated a rule-based model that predicted a value for each pixel, and all committee model predictions were averaged for a final predicted pixel value (RuleQuest, 2008). The regression-tree model output file included model parameters that were input, along with spatial rasters of the independent variables, into a mapping application. The ACP model was applied to respective time-dependent data (eMODIS derivatives) to map respective year ACP.

Validation

Of the original dataset, 4 012 random points were used to test the model's predictive accuracy. For both training and test data, Cubist output an average error, a relative error, and a correlation of coefficient

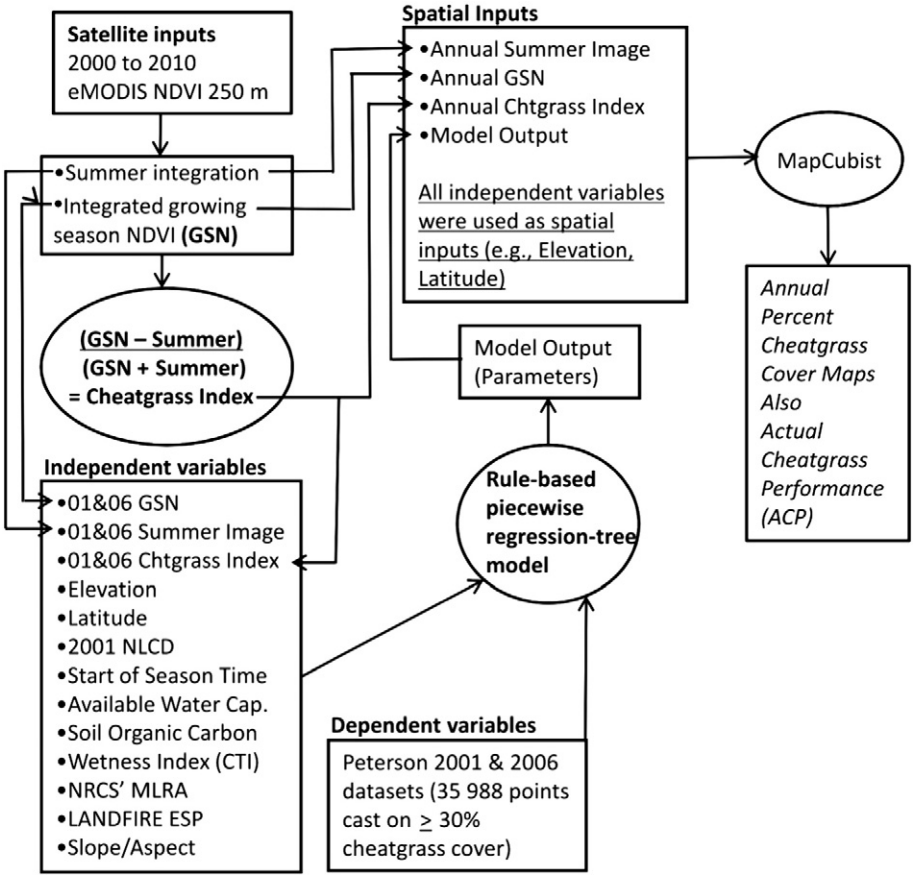

Fig. 1. The modeling process and data used to generate the cheatgrass percent cover (ACP) time series of maps.

statistic. A relative error magnitude was the ratio of the average error magnitude compared with the error magnitude that resulted from always predicting the mean value. A relative error of less than 1.0 indicated that the model was useful for predicting cheatgrass percent cover (RuleQuest, 2008).

Expected Cheatgrass Performance

The ACP estimates served as the dependent variable in the ECP model. Overperforming pixels had significantly higher cheatgrass percent cover than the model expected, and underperforming pixels had significantly less cheatgrass percent cover than the model expected. The ECP model was used to develop a time series of annual ECP estimates. Independent variables in the ECP model included site potential and PRISM weather data (PRISM Climate Group, Oregon State University, http://www.prism.climate.org) parsed into five seasonal datasets. Site potential represented the long-term cheatgrass percent cover and captured this metric's spatial variability without consideration for annual weather variation, disturbances, or effects of management activities. Including weather data as an independent variable detrended the model for weather and added annual variability to the modeling output. The ECP model output was, along with the gridded seasonal weather data and a raster of the site potential dataset, input into MapCubist as described in the ACP earlier to generate annual ECP maps from 2000–2010.

The ECP model was trained on 38 245 points from the time series of cheatgrass percent cover datasets (ACP). These points were stratified to include approximately equal numbers of points from each year in our time series. To build a model that represented a range of cheatgrass percent cover, points were stratified randomly into five classes on the basis of cheatgrass percent cover: zero, 1 to 12, 13 to 25, 25 to 50, and more than 50. These points were trained on areas where the 2001 NLCD identified the land cover as grassland/herbaceous or shrub and at elevations equal to 2000 m or lower.

Cubist software was used to predict cheatgrass percent cover on the basis of PRISM weather data and site potential. Figure 2 illustrates the modeling process and data used to estimate cheatgrass percent cover. We built a predictive model that used a committee of 3 with 55 rules. After the model file was developed, the file along with the seasonal weather data and site potential rasters were input into MapCubist to develop the time series of ECP maps.

Ecosystem Performance Anomalies

Cheatgrass performance anomalies could occur at a given site 1 year and not the next, or they could persist at a site for several consecutive years (M. Zielinski, personal communication, September, 2010). Because dieoffs are spatially and temporally variable, we chose to classify a pixel as dieoff only if it underperformed at least 2 consecutive years. Ecosystem performance anomalies provided annual datasets that identified areas where cheatgrass performed as expected at the 80% confidence level (normal performance), significantly greater than expected (overperformance), or significantly less than expected (underperformance). Underperforming areas likely represented cheatgrass dieoff, although in some cases effects from early spring grazing, a fire from the previous year, or management activities like seeding with native species could have been classified as underperformance.

Fire Chronosequence

To understand the effect of fire on cheatgrass performance, random points were cast inside fire polygons that burned in the study area from 1997–2010. These polygons were downloaded from the Monitoring Trends in the Burn Severity (MTBS) website.[7] Random points were removed if they were cast where the mask had been applied. A total of 17 050 random points were used. We extracted values from the 2000–2010 ecosystem performance anomaly maps for all random points. A total of 116 835 values were extracted and categorized according to time before or since fire.

[7] http://www.mtbs.com/.

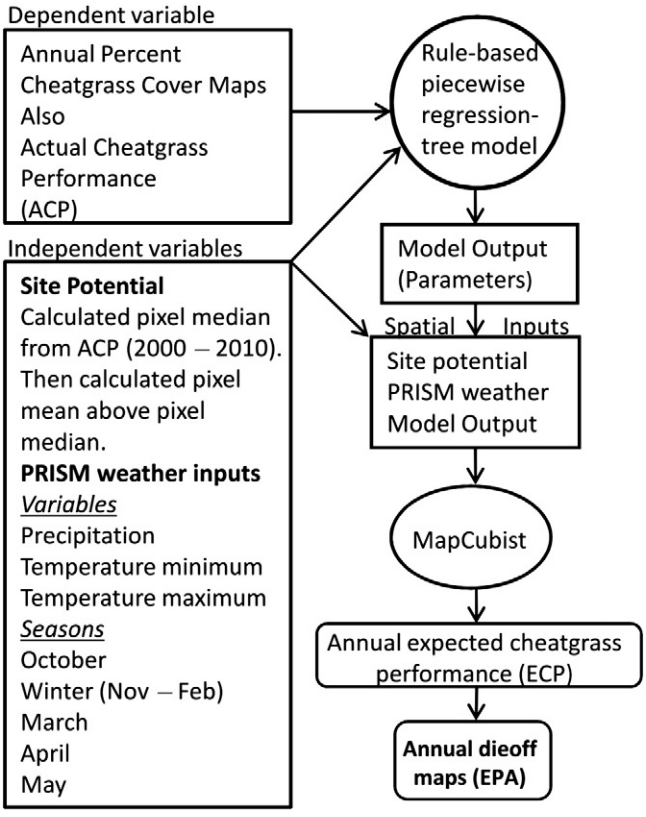

Fig. 2. The modeling process and data used to generate the expected cheatgrass performance (ECP) time series of maps.

Validation

Of the original dataset, 4 296 random points were used to test the model's predictive accuracy. The cheatgrass performance anomaly dataset was validated using polygons created by the BLM on the basis of helicopter flights during early 2010 to identify areas of

Table 1
Driving variables for cheatgrass start of spring growth model and model accuracy. Frequency of usage (%) is displayed for each variable for model stratification and prediction. Dashes indicate variable not used.

Driving variable	Stratification	Prediction
Start of season time (SOST)	68	83
Latitude	31	24
March temperature maximum (t_{max})	31	84
October precipitation (ppt)	26	24
April t_{max}	10	66
April temperature minimum (t_{min})	6	50
April ppt	2	51
March ppt	1	44
Soil organic carbon	–	47
Available water capacity	–	44
Winter ppt	–	44
Winter t_{max}	–	29
October t_{min}	–	23

Training data $R^2 = 0.71$. RMSE = 3.07. Average error = 1.4 weeks. Relative error = 0.48 week.
Test data $R^2 = 0.44$. RMSE = 2.69. Average error = 1.8 weeks. Relative error = 0.63 week.

Table 2
Driving variables for cheatgrass percent cover model (ACP). Frequency of usage (%) is displayed for each variable. Dashes indicate variable was not used (3-committee model with limit of 100 rules).

Driving variable	Stratification	Prediction
Elevation	84	93
Latitude	73	76
Cheatgrass index	63	72
Spring period	63	96
Summer period	36	86
2001 NLCD	31	–
Start of season time	25	56
MLRA	17	–
CTI	12	62
Available water capacity	11	58
LANDFIRE ESP	7	–
Soil Organic Carbon	–	46
Steep slope south	–	23
Steep slope north	–	31

Training data $R^2 = 0.84$. RMSE = 6.91. Average error = 4.4%. Relative error = 0.33%. Test data $R^2 = 0.83$. RMSE = 6.28. Average error = 4.6%. Relative error = 0.34%.

Table 3
Driving variables for cheatgrass performance model and model accuracy. Frequency of usage (%) is displayed for each variable. Dashes indicate variable was not used.

Driving variable	Stratification	Prediction
Site potential	100	99
May temperature maximum (t_{max})	39	57
April t_{max}	20	50
Winter t_{max}	18	63
May precipitation (ppt)	17	56
April ppt	17	34
March ppt	12	24
October t_{max}	11	67
March t_{max}	11	76
Winter ppt	6	26
October ppt	6	45
March temperature minimum (t_{min})	4	75
April t_{min}	2	32
Winter t_{min}	–	59
October t_{min}	–	55
May t_{min}	–	61

Training data $R^2 = 0.88$. RMSE = 6.95. Average error = 3.4%. Relative error = 0.30%. Test data $R^2 = 0.86$. RMSE = 5.75. Average error = 3.7%. Relative error = 0.32%.

cheatgrass dieoff. Dieoff polygons were overlain onto the 2009 ecosystem performance map. The map was assessed for underperformance inside and outside of the polygons.

Results

Cheatgrass Start of Spring Growth

Table 1 shows all independent variables used to build the cheatgrass start of spring growth model and the frequency that each variable was used to develop rules for stratification and in associated prediction algorithms. The SOST variable was used most often to stratify the model's rules, and it was used second most often in the prediction algorithms. Other important variables were March temperature maximum (t_{max}) and April t_{max}. April variables were used most frequently, suggesting that April weather was most important for cheatgrass start of spring growth for this study area. The accuracy for the 939 training points was relatively strong ($R^2 = 0.71$). The accuracy for 99 test points was more modest ($R^2 = 0.44$).

Actual Cheatgrass Performance

Table 2 shows all independent variables used to develop the actual cheatgrass performance model. In this model, we did not include weather data because the growing season NDVI used a dynamic start of season variable to capture most weather effects. Elevation was used most frequently for stratifying rules and second most often in creating the prediction algorithms. Latitude was also important in creating the model. Three variables developed using eMODIS data (i.e., the cheatgrass index and the spring and summer periods) were important driving variables in model development. The strong usage of the index and the two periods demonstrated the importance of remote sensing data to understanding cheatgrass cover dynamics using a regression-tree model approach. The NLCD, LANDFIRE, and MLRA datasets provided the model with discrete variables and, therefore, were only used by the model to stratify its rules. The soils data (i.e., available water capacity and soil organic carbon) contributions to the model were relatively strong.

The training data ($n = 35\,988$) R^2 value was strong at 0.84. The test data ($n = 4\,012$) R^2 value was also strong at 0.83. Test data relationships usually are weaker than training data relationships because the R^2 statistic is sensitive to the range and distributions of the data values. The training and test dataset R^2 values were almost identical, indicating a robust model. The RMSEs for the training and test data were similar. The relative errors of both the training and test data were substantially less than one, showing that a useful model was developed.

Figure 3 displays data from the 2001 and 2006 cheatgrass percent cover maps plotted against our predicted cheatgrass percent cover (ACP) training data. Data points were mostly clustered around the regression line, illustrating the strong relationship between datasets. The 1:1 line lies above the regression line through most of the scatterplot, indicating that the model tended to underestimate cheatgrass percent cover at values above about 20, although a low proportion of points

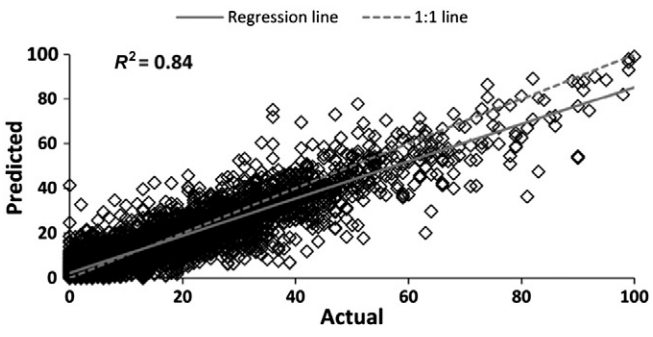

Fig. 3. The predicted (modeled) ACP training dataset regressed on the 2001 and 2006 cheatgrass percent cover datasets. The 1:1 line represents the equation y = x. The results of this model were extrapolated to the entire Northern Great Basin for 11 years.

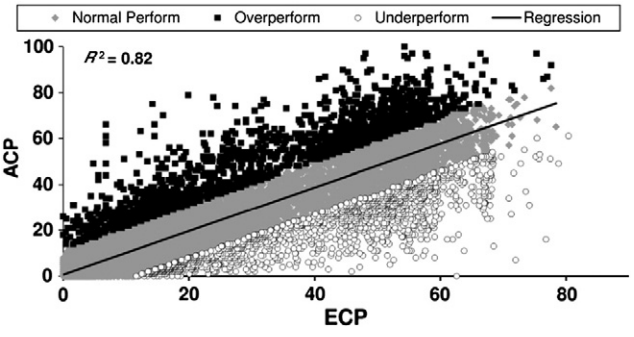

Fig. 4. Training data from actual cheatgrass performance (ACP) regressed on training data from expected cheatgrass performance (ECP) with the regression line and the 80% confidence limits displayed. The confidence limits were used to establish significant model anomalies. Pixels that burned the immediate previous year were excluded from training data.

was represented where percent cover underestimation was greatest at the extreme upper end of the scatterplot. The points that resided farthest from the regression line in the middle portion of the scatterplot were more evenly distributed between overestimating and underestimating cheatgrass percent cover. The model accuracy below about 25% cheatgrass cover was extremely strong.

Expected cheatgrass performance

The cheatgrass performance model, a function of site potential and weather, was a 3-committee model limited to 55 rules. The independent variables used to develop the cheatgrass performance model and their usage levels are shown in Table 3. Site potential, the variable that represented the long-term spatial average for cheatgrass, was used both for stratification of the rules and development of the prediction algorithms in most cases. This strong use of site potential suggested that cheatgrass performance was highly dependent on location. Other variables used to develop the performance model were weather variables that contributed interannual variation to the model. The weather variables were used at different frequencies in the model, both to stratify the rules and to develop the prediction algorithms. March t_{min} and t_{max} variables were used sparingly to stratify the rules, but they were used in at least 75% of prediction algorithms. All May weather variables figured relatively prominently in the development of the prediction algorithms. Considering all April weather variables were used in the development of at least 50% of all cheatgrass start of spring growth model prediction algorithms (see Table 1), the relatively strong use of May weather variables in the performance model was expected as a short time lag should exist between cheatgrass start of spring season and cheatgrass peak performance because it was a short-lived grass. The performance model proved to be robust with its training data ($n = 38\,245$; $R^2 = 0.88$) and test data ($n = 4\,296$; $R^2 = 0.86$). The training and test data experienced relative errors below one. The RMSE values were relatively comparable.

In Figure 4, we plotted ECP training data against ACP training data, and the distances from each point and the regression line represented the model residual. These residuals included the model error, but the error should have fallen mostly within the 80% confidence interval. Residuals that fell outside of the confidence interval represented significant anomalies, or EPAs. Diamonds near the regression line that fell within the confidence interval were normal performing pixels, squares above the regression line that fell outside the confidence interval represented overperforming pixels, and circles below the regression line that fell outside the confidence interval represented underperforming pixels. Each point represented a pixel for one particular year during the study period, so any one pixel could be represented by all three classes as it could have moved from normal performing to

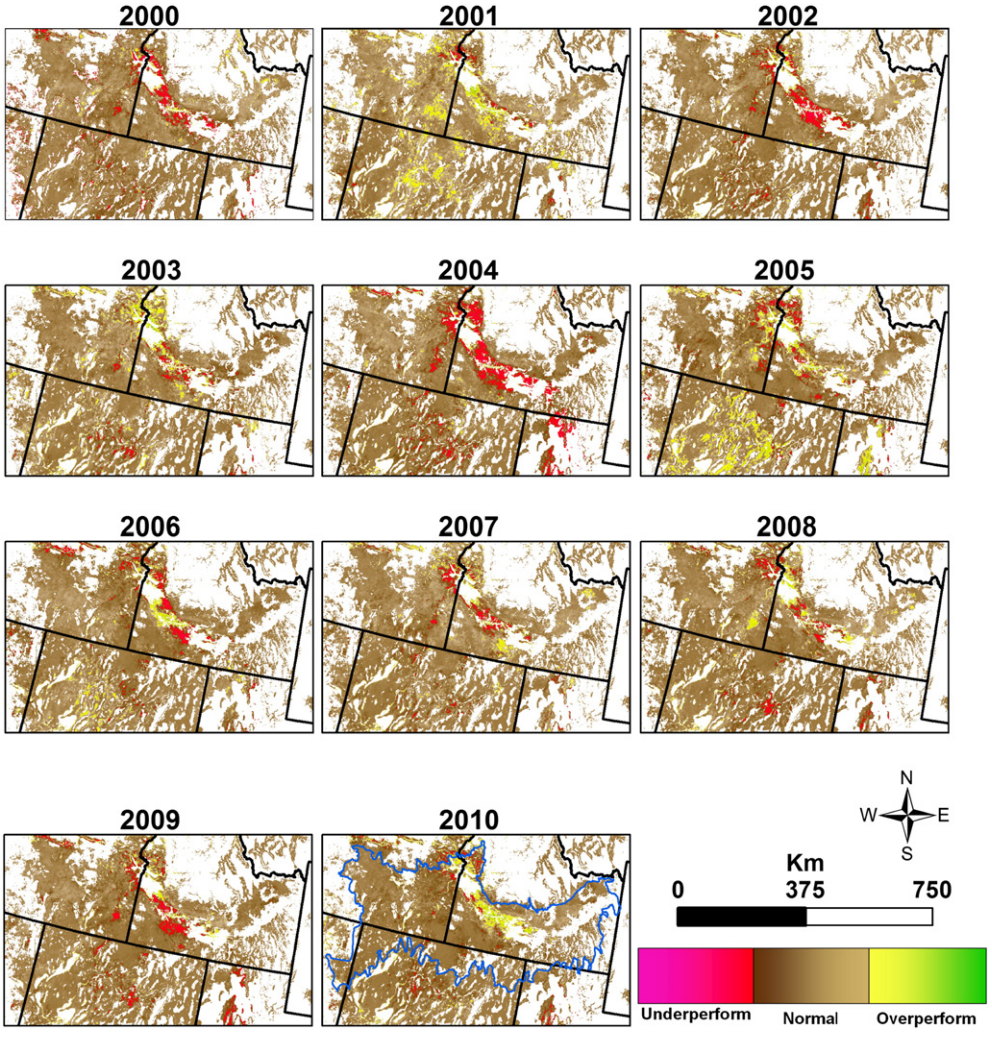

Fig. 5. Cheatgrass ecosystem performance anomaly maps for 2000–2010. The 2010 map displays the Northern Great Basin boundary. Overperformance indicates where cheatgrass performance exceeded model expectations. Normal performing areas show where cheatgrass performed within the model's 80% confidence interval. Underperforming pixels indicate where cheatgrass performance did not meet model expectations and represented possible cheatgrass dieoff.

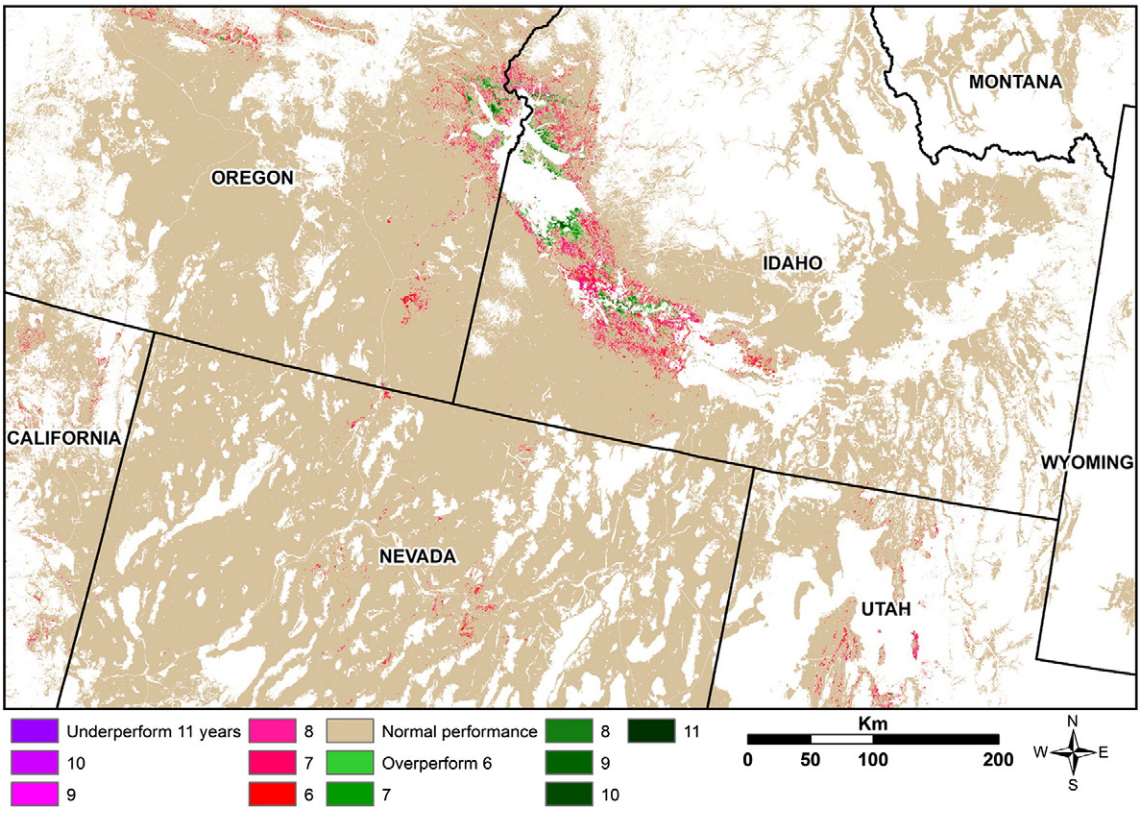

Fig. 6. The cheatgrass persistent anomaly map shows areas in the Northern Great Basin that underperformed at least 6 of 11 years, overperformed for at least 6 of 11 years, or demonstrated patterns of normal performance during the study period.

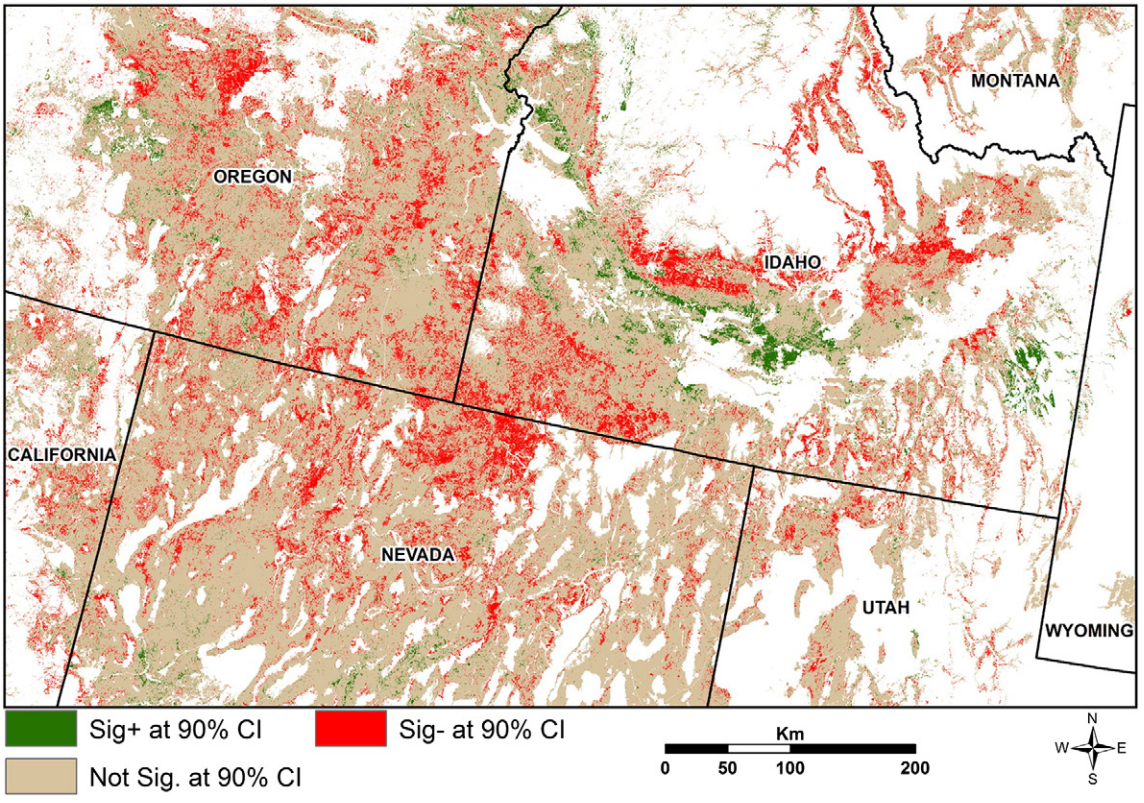

Fig. 7. The trend map highlights areas in the Northern Great Basin where positive and negative significance values of the slope coefficient of EPA at the 90% confidence interval is regressed on years for each pixel.

Table 4
Mean values for potential drivers of cheatgrass performance persistent anomaly classes and normal performance are displayed in the table. The climate data are based on PRISM annual 30-year averages (1981–2010). Available water capacity (AWC) and soil organic carbon (SOC) are NRCS SSURGO datasets.

Class	Area (km^2)	Elevation (m)	Cheat Cover (%)	Cheat Cover CV	PPT (mm)	T_{max} °C	T_{min} °C	AWC (cm)	SOC (kg.m-2)
Normal	262 491	1 535	13.62*	48.79	324	15.02	0.33	3.79	2.37
Overperform	1 257	891	57.28	23.25	298	16.88	2.57	4.57	2.65
Underperform	4 827	1 106	53	47.78	316	16.43	1.86	4.19	2.58

* This value excludes pixels with cheatgrass cover less than 5% to compensate for difficulty in distinguishing between bare ground and low vegetation cover.

underperforming to overperforming and then back to any of the classes through time. As a point moved on the chart, horizontal movement reflected the effects from weather and vertical movement reflected the effects from disturbances and management activities.

Figure 5 displays cheatgrass ecosystem performance anomaly maps for each year during the study period (2000–2010). Areas on the maps of cheatgrass overperformance show where cheatgrass performed better than our model expected. Normal performing areas show where cheatgrass performed within the model's 80% confidence interval. Underperforming pixels represented areas where cheatgrass performed worse than our model expected and represented possible cheatgrass dieoff. Other factors could have affected cheatgrass performance that may not be related to cheatgrass dieoff, such as cheatgrass used as early-season forage for livestock. The maps reflect changing performance from year to year. Some areas consistently underperformed while other areas consistently overperformed. Expected cheatgrass performance was highly dynamic in the Snake River Plain in north-central Nevada and northwestern Utah.

Ecosystem performance: persistent anomalies and trends

Figure 6 highlights persistent anomalies in the study area. To be classified as persistent, a pixel must have *over*performed at least 6 of the 11 years or *under*performed at least 6 of the 11 years during the study period (2000–2010). The Snake River Plain, which extends from eastern Oregon to southwestern Idaho, contained the majority of persistent anomalies. Outside of the Snake River Plain, almost all persistent anomalies were underperforming. Figure 7 shows the EPA trend through time. This map was based on the direction of the anomaly trend and the slope of the trend's regression. Trends that were not significant at the 90% confidence level equaled 82% of the study area. Significantly negative trends (decreasing conditions when weather and site variation are accounted for) at the 90% confidence level were more common (15% of the study area) than significantly positive trends (3%) (increasing conditions when weather and site variation are accounted for).

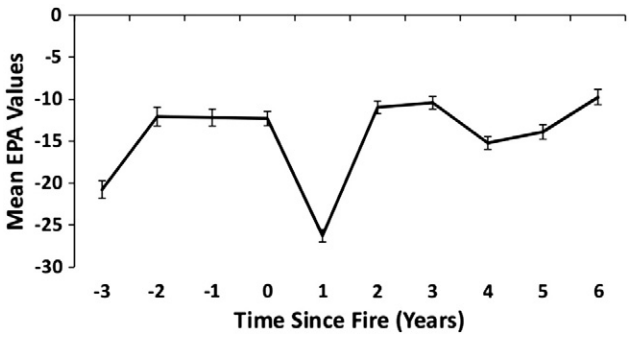

Fig. 8. The effects of fire on cheatgrass performance show the mean cheatgrass EPA values of 17 050 pixels for up to 3 years before a fire, the year of a fire, and up to 6 years after a fire. The standard error of the mean is displayed as whiskers on the graph. Data are from a sample of 1 295 fires that burned from 1997 to 2010 in the study area.

Table 4 shows mean values for potentially important drivers of cheatgrass performance cross referenced with our persistent anomaly dataset for each performance class. Persistently normal performing pixels covered almost the entire unmasked portion of our study area (98%); consequently, the spatial variation of this class was much greater than the other two classes. This finding is expected because of the relatively rigorous definition of what qualifies as a persistent anomaly and because most of the study area had not experienced cheatgrass dieoff. Persistently overperforming pixels covered less than 1% of the study area, and persistently underperforming pixels covered about 2%. On average, overperforming pixels were located in the Snake River Plain and at sites that were drier and warmer and at lower elevations than underperforming and normal performing pixels. These overperforming sites experienced higher average cheatgrass percent cover than sites representing the other two classes, but with half of the annual variability. Also, these sites typically had better soils with available water capacity and soil organic carbon mean values slightly higher than sites of the other classes. The underperforming anomalies occupied an elevational niche between the normal and overperforming classes and, as a result, experienced long-term average annual precipitation and temperatures that also fell between these two classes. The average cheatgrass percent cover of underperforming sites was similar to overperforming sites, but the annual variability of underperforming sites, or coefficient of variation (CV), was more than double and almost equal to the CV of normal performing sites.

Fire chronosequence

For each time-since-fire category, we calculated the mean ecosystem performance anomaly value and displayed that data as a line graph in Figure 8. We also calculated the standard error of the mean and displayed that data as whiskers. Postfire cheatgrass performance varies substantially depending on circumstances like location characteristics, fire characteristics, postfire nitrogen availability, and management treatments. This variation caused a wide range of ecosystem performance anomaly values within individual fires and among fires. Therefore understanding average cheatgrass ecosystem performance anomaly values postfire can be valuable.

Figure 8 shows that during the first year since fire, cheatgrass performance experienced a significant decline from the previous 3 years when cheatgrass EPA values were stable. Three years before fire, average cheatgrass EPA was lower than all other years except for the first year since fire. Cheatgrass performance experienced a significant increase during the second year since fire, stabilized for 1 year, and then began fluctuating modestly during years 4 through 6 since fire. The highest cheatgrass ecosystem performance anomaly values occurred during years 2, 3, and 6 since fire. Mean values for all categories were negative, although they all fell in the normal performing range.

Validation

We validated the ecosystem performance anomaly maps using a dataset provided by the Winnemucca District Office of the BLM. During spring 2010, the BLM conducted helicopter flights to map areas previously identified as possible cheatgrass dieoff in the Winnemucca

District. A set of dieoff polygons were developed. We compared the polygons to our 2009 ecosystem performance anomaly map, limiting analysis to the area within the Winnemucca District. We found 41% of the pixels inside of these polygons were classified as possible dieoff pixels, 58% were normal performing, and 1% were classified as overperforming. Outside of the dieoff polygons, 2% of the pixels were classified as possible dieoffs, 97% were normal performing, and 1% were classified as overperforming. Requiring a pixel to experience 2 consecutive years of underperformance to qualify as a dieoff likely contributed to a lower percentage of underperforming pixels being located within the dieoff polygons. The substantially lower percentage of pixels classified as underperforming outside of the polygons as opposed to inside of the polygons speaks to the accuracy of this modeling process and the annual EPA maps.

Discussion

The current study provides a landscape-scale understanding of cheatgrass performance dynamics, focused on cheatgrass dieoff. We analyzed the relationships between cheatgrass performance and landscape and environmental variables, and the information discovered can be useful to land managers when they develop management strategies and assess treatment effectiveness. Bradley and Mustard (2005) and Clinton et al. (2010) used satellite imagery and precipitation data to accurately identify cheatgrass. Bradley and Mustard (2005) documented a magnification of cheatgrass production compared with native plant production during years of high precipitation when compared with years with low precipitation. Our cheatgrass performance results needed to be consistently interpretable, so we employed the dynamic monitoring of ecosystem performance approach so that cheatgrass percent cover (ACP) was measured relative to weather and, therefore, effects from disturbances and management activities stand out as anomalies.

The cheatgrass start of spring growth model produced a spatially dynamic phenology guideline to parameterize the cheatgrass growing season (Boyte et al., 2013). Because of the seasonality of cheatgrass response to weather and the study area's relatively wide elevational and latitudinal ranges, this model's strong use of certain weather variables in the prediction algorithm was expected. With a relatively broad start of season period, March and April temperature maximums (Young et al., 1987; Leffler et al., 2011) and precipitation events should have been critical for the start of cheatgrass growth over much of this area. Cheatgrass is a C_3 grass that, while able to germinate during fall or spring and develop roots during winter, developed shoots during spring (Leffler et al., 2011). Winter precipitation events that occurred as snow and melted during late winter or early spring would have also been relatively important for cheatgrass start of spring growth, providing much-needed early-season moisture.

The ACP dataset included the effects of weather, site potential, land management, and disturbances. Elevation and latitude were also used heavily to develop the ACP dataset. These two variables helped determine the likelihood of cheatgrass presence because they strongly influenced weather, and weather was an important factor in cheatgrass establishment and performance in the Northern Great Basin (Bradley and Mustard, 2006; Chambers et al., 2007). The ECP model separated land management and disturbances from influences of weather and site potential, making the comparison between ACP and ECP outputs more directly interpretable. The ECP model normalized for weather and facilitated interannual comparisons and analysis. We developed this model so that it was not trained on areas that experienced a fire during the previous year, so measurement of cheatgrass performance would not be strongly influenced by fire effects (Young and Evans, 1978; Johnson et al., 2011; Ellsworth and Boone Kauffman, 2013). The extremely strong use of site potential in model development suggested that cheatgrass performance was strongly driven by spatial factors like the presence of cheatgrass seed or a fungus like the black fingers of death. Also, competition, or lack thereof, from other vegetation types would have affected cheatgrass performance (Chambers et al., 2007).

The comparisons of performance classes to cheatgrass percent cover and landscape and environmental characteristics revealed that areas of persistent cheatgrass underperformance were, on average, at higher elevations, more mesic, cooler, and located on sites that had poorer soils than areas of persistent cheatgrass overperformance. The average cheatgrass percent cover was similar between the two classes. However, the coefficient of variation (CV) statistic indicated that annual variability of cheatgrass percent cover for the overperformance class was substantially lower than that of the underperformance and normal performance classes. One BLM employee from the Winnemucca District observed areas of cheatgrass dieoff that were followed 2 to 3 years later by the return of cheatgrass and then subsequent dieoffs (M. Zielinski, personal communication, September, 2010). This dieoff dynamic could explain the higher CV value for underperforming pixels even though the underperforming and normal-performing CVs were similar; therefore the explanation for the disparity in CV values for classes likely lies within the overperforming class where environmental variables could be conducive to more consistent cheatgrass performance.

Fire killed both cheatgrass seed and the black fingers of death fungus, but it did not necessarily kill all seeds or all of the fungus (Beckstead et al., 2011). Fewer seeds available for germination would mean less cheatgrass postfire, and this phenomenon was observed (Mealor et al., 2012) during the first year postfire in high elevations of the sagebrush steppe and the pine forest in central Wyoming. Young and Evans (1978) also noted a reduction in cheatgrass density during the first year postfire in the central Northern Great Basin, although they found that individual plant vigor was extremely high, and cheatgrass density increased substantially in subsequent years. Our fire chronosequence showed that average EPA values declined 1 year postfire but rebounded to greater than prefire levels during the second year after fire, perhaps reflecting increased seed sources resulting from increased plant vigor. Rigge et al. (2013) noted a decline in ecosystem performance anomaly values in the Greater Platte River and Upper Colorado River basins grasslands until 3 years after fire. Ecosystem performance anomaly values did not return to preburn values until about 6 years postfire. Cheatgrass was not identified as a part of that study's grassland cover, and most of the grassland fires analyzed occurred in the Great Plains. Nitrogen increases (Moorhead et al., 1988; Johnson et al., 2011) and the recovery of cheatgrass seed banks 1-year postfire (Ellsworth and Boone Kauffman, 2013) can be explanations for increased ecosystem performance anomaly values during the second year postfire. This regional summarization may indicate that the time period for optimal cheatgrass control could be within the first year after the fire. The postfire boost in cheatgrass primarily during the second and third years postfire may indicate these are critical years of fine fuel buildup, which increases wildfire probabilities.

Management Implications

The ecosystem change caused by cheatgrass dieoff in the Northern Great Basin presents new management challenges (i.e., increased soil erosion, possibilities of the introduction of weed species new to the area, and loss of early spring forage for both livestock and wildlife). It also could present new opportunities for native species restoration or the inclusion or expansion of species that may add value to the land. However, the dieoff phenomenon is not well understood. A crucial part of understanding dieoff dynamics was identifying areas of cheatgrass dieoff at a landscape scale, especially areas of persistent

or reoccurring dieoffs. Analyzing the relationships between dieoffs and landscape and environmental characteristics also could provide valuable information. This study provided the information to begin conducting these analyses, allowing land managers to explore opportunities for mitigating cheatgrass dieoff and possibly develop new strategies for managing western rangelands.

The landscape-scale monitoring study presented here identified cheatgrass dieoff for 11 years, thus furthering knowledge about recent rangeland dynamics. We separated annual weather variation from the influences of disturbances and management, which allowed us to map possible dieoffs as underperforming anomalies. This technique has been used successfully in other landscapes for other studies. Applied to a rangeland environment experiencing cheatgrass dieoff, this technique allowed a clearer picture to emerge about where cheatgrass dieoff may have occurred and where land management activities, or at least further research, may be necessary.

Acknowledgements

The authors thank Matthew Rigge, Thomas Adamson, and two anonymous reviewers for their reviews of this manuscript. Their comments have made this a better and more readable paper. We also acknowledge Lei Ji for developing the performance trend model and Kari Beckendorf for her assistance with processing data layers.

References

Balch, J.K., Bradley, B.A., D'Antonio, C.M., Gómez-Dans, J., 2013. Introduced annual grass increases regional fire activity across the arid western USA (1980–2009). Global Change Biology 19, 173–183.

Baynes, M., Newcombe, G., Dixon, L., Castlebury, L., O'Donnell, K., 2012. A novel plant-fungal mutualism associated with fire. Fungal Biology 116, 133–144.

Beckstead, J., Meyer, S.E., Molder, C.J., Smith, C., 2007. A race for survival: can *Bromus tectorum* seeds escape *Pyrenophora semeniperda*–caused mortality by germinating quickly? Annals of Botany 99, 907–914.

Beckstead, J., Meyer, S.E., Connolly, B.M., Huck, M.B., Street, L.E., 2010. Cheatgrass facilitates spillover of a seed bank pathogen onto native grass species. Journal of Ecology 98, 168–177.

Beckstead, J., Street, L.E., Meyer, S.E., Allen, P.S., 2011. Fire effects on the cheatgrass seed bank pathogen *Pyrenophora semeniperda*. Rangeland Ecology & Management 64, 148–157.

Boyte, S.P., Wylie, B.K., Major, D.J., Brown, J.F., 2013. The integration of geophysical and enhanced Moderate Resolution Imaging Spectroradiometer Normalized Difference Vegetation Index data into a rule-based, piecewise regression-tree model to estimate cheatgrass beginning of spring growth. International Journal of Digital Earth http://dx.doi.org/10.1080/17538947.2013.860196.

Bradley, B.A., Mustard, J.F., 2005. Identifying land cover variability distinct from land cover change: cheatgrass in the Great Basin. Remote Sensing of Environment 94, 204–213.

Bradley, B.A., Mustard, J.F., 2006. Characterizing the landscape dynamics of an invasive plant and risk of invasion using remote sensing. Ecological Applications 16, 1132–1147.

Bromberg, J.E., Kumar, S., Brown, C.S., Stohlgren, T.J., 2011. Distributional changes and range predictions of downy brome *(Bromus tectorum)* in Rocky Mountain National Park. Invasive Plant Science and Management 4, 173–182.

Chambers, J.C., Roundy, B.A., Blank, R.R., Meyer, S.E., Whittaker, A., 2007. What makes Great Basin sagebrush ecosystems invasible by *Bromus tectorum*? Ecol Monogr 77, 117–145.

Chaplot, V., Walter, C., 2003. Subsurface topography to enhance the prediction of the spatial distribution of soil wetness. Hydrological Processes 17, 2567–2580.

Clinton, N.E., Potter, C., Crabtree, B., Genovese, V., Gross, P., Gong, P., 2010. Remote sensing-based time-series analysis of cheatgrass (*Bromus tectorum* L.) phenology. J Environ Qual 39, 955–963.

De'ath, G., Fabricius, K.E., 2000. Classification and regression trees: a powerful yet simple technique for ecological data analysis. Ecology 81, 3178–3192.

Ellsworth, L.M., Boone Kauffman, J., 2013. Seedbank responses to spring and fall prescribed fire in mountain big sagebrush ecosystems of differing ecological condition at Lava Beds National Monument, California. Journal of Arid Environments 96, 1–8.

Goergen, E.M., Leger, E.A., Espeland, E.K., 2011. Native perennial grasses show evolutionary response to *Bromus tectorum* (cheatgrass) invasion. PLoS One 6, 1–8.

Gu, Y., Brown, J.F., Miura, T., van Leeuwen, W.J., Reed, B.C., 2010. Phenological classification of the United States: a geographic framework for extending multi-sensor time-series data. Remote Sensing 2, 526–544.

Gu, Y., Boyte, S.P., Wylie, B.K., Tieszen, L.L., 2012. Identifying grasslands suitable for cellulosic feedstock crops in the Greater Platte River basin-dynamic modeling of ecosystem performance with 250-m eMODIS. Global Change Biology Bioenergy 4, 96–106.

Jenkerson, C.B., Maiersperger, T.K., Schmidt, G.L., 2010. eMODIS-a user-friendly data source. *U.S. Geological Survey Open-File Report 2010–1055*.

Johnson, B.G., Johnson, D.W., Chambers, J.C., Blank, R.R., 2011. Fire effects on the mobilization and uptake of nitrogen by cheatgrass (*Bromus tectorum* L.). Plant and Soil 341, 437–445.

Kokaly, R.F., 2011. DESI—Detection of early-season invasives (software-installation manual and user's guide version 1.0). U.S. Geological Survey Open-File Report 2010-1302: Reston, VA.

Leffler, A.J., Monaco, T.A., James, J.J., 2011. Nitrogen acquisition by annual and perennial grass seedlings: testing the roles of performance and plasticity to explain plant invasion. Plant Ecology 212, 1601–1611.

Link, S.O., Gee, G.W., Downs, J.L., 1990. The effect of water stress on phenological and ecophysiological characteristics of cheatgrass and Sandberg's bluegrass. J Range Manage 43, 506–513.

Mack, R.N., 2011. Fifty years of 'waging war on cheatgrass': research advances, while meaningful control languishes. In: Richardson, D.M. (Ed.), Fifty years of invasion ecology: the legacy of Charles Elton. Blackwell Publishing Ltd., Oxford, UK, pp. 253–265.

Mack, R.N., Pyke, D.A., 1983. The demography of Bromus tectorum: variation in time and space. J of Ecol 71, 69–93.

Mealor, B.A., Cox, S., Booth, D.T., 2012. Postfire downy brome *(Bromus tectorum)* invasion at high elevations in Wyoming. Invasive Plant Science and Management 5, 427–435.

Meyer, S.E., Quinney, D., Nelson, D.L., Weaver, J., 2007. Impact of the pathogen *Pyrenophora semeniperda* on *Bromus tectorum* seedbank dynamics in North American cold deserts. Weed Research 47, 54–62.

Moorhead, D.L., Fisher, F.M., Whitford, W.G., 1988. Cover of spring annuals on nitrogen-rich kangaroo rat mounds in a Chihuahuan Desert grassland. American Midland Naturalist 120, 443–447.

Peterson, E.B., 2005. Estimating cover of an invasive grass *(Bromus tectorum)* using tobit regression and phenology derived from two dates of Landsat ETM + data. Int J Remote Sens 26, 2491–2507.

Peterson, E.B., 2007. A map of annual grasses in the Owyhee Uplands, Spring 2006, derived from multitemporal Landsat 5 TM imagery. U.S. Department of Interior, Bureau of Land Management, Nevada State Office, Reno, Carson City, Nevada.

Reed, B.C., Brown, J.F., Vanderzee, D., Loveland, T.R., Merchant, J.W., Ohlen, D.O., 1994. Measuring phenological variability from satellite imagery. Journal of Vegetation Science 5, 703–714.

Rigge, M., Wylie, B.K., Gu, Y., Belnap, J., Phuyal, K., Tieszen, L.L., 2013. Monitoring the status of forests and rangelands in the Western United States using ecosystem performance anomalies. International Journal of Remote Sensing 34, 4049–4068.

RuleQuest, 2008. An overview of Cubist, from http://www.rulequest.com/cubist-win.html. RuleQuest Pty Ltd., St. Ives NSW 2075, Australia.

Salo, C., 2011. Land lines. Rangelands 33, 60–62.

Swets, D.L., Reed, B.C., Rowland, J.D., Marko, S.E., 2000. A weighted least-squares approach to temporal NDVI smoothing. Proceedings of the 1999 ASPRS Annual Conference, From Image to Information. Portland, OR, 17–21 May 1999: American Society for Photogrammetry and Remote Sensing.

Toms, J., Lesperance, M.L., 2003. Piecewise regression: a tool for identifying ecological thresholds. Ecology 84, 2034–2041.

U.S. Department of Interior, B. L. M., 2010. Rapid ecological assessment of the Northern Great Basin and Range and Snake River Plain. BLM/OC/ST-10/002+1636, Denver, CO, p. 43.

West, N.E., Young, J.A., 2000. Intermountain valleys and lower mountain slopes. In: Barbour, M.G., Billings, D. (Eds.), North American terrestial vegetation, 2nd edition Cambridge University Press, Cambridge, UK, pp. 256–284.

Whisenant, S.G., 1990. Changing fire frequencies on Idaho's Snake River Plains: ecological and management implications. INT-276. USDA, Ogden, UT, USA, pp. 4–10.

White, M.A., de Beurs, K.M., Didan, K., Inouye, D.W., Richardson, A.D., Jensen, O.P., O'Keefe, J., Zhang, G., Neman, R.R., van Leeuwen, W.J.D., Brown, J.F., De Wit, A., Schaepman, M., Lin, X., Dettinger, M., Bailey, A.S., Kimball, J., Schwartz, M.D., Baldocchi, D.D., Lee, J.T., Lauenroth, W.K., 2009. Intercomparison, interpretation, and assessment of spring phenology in North America estimated from remote sensing for 1982–2006. Global Change Biology 15, 2335–2359.

Wiken, E., Nava, F.J., Griffith, G., 2011. North American Terrestrial Ecoregions-Level III. Commission for Environmental Cooperation, Montreal, Canada.

Wylie, B.K., Fosnight, E.A., Gilmanov, T.G., Frank, A.B., Morgan, J.A., Haferkamp, M.R., Meyers, T.P., 2007. Adaptive data-driven models for estimating carbon fluxes in the Northern Great Plains. Remote Sensing of Environment 106, 399–413.

Wylie, B.K., Zhang, L., Bliss, N., Ji, L., Tieszen, L.L., Jolly, W.M., 2008. Integrating modelling and remote sensing to identify ecosystem performance anomalies in the boreal forest, Yukon River Basin, Alaska. International Journal of Digital Earth 1, 196–220.

Wylie, B.K., Boyte, S.P., Major, D.J., 2012. Ecosystem performance monitoring of rangelands by integrating modeling and remote sensing. Rangeland Ecology & Management 65, 241–252.

Young, J.A., Evans, R.A., 1978. Population dynamics after wildfire in sagebrush grasslands. Journal of Range Management 31, 283–289.

Young, J.A., Evans, R.A., Eckert, R.E.J., Kay, B.L., 1987. Cheatgrass. Rangelands 9, 266–270.

Zielinski, M., personal, communication, September 2010.